Searchlight and Doppler Effects in the Visualization of Special Relativity: A Corrected Derivation of the Transformation of Radiance

DANIEL WEISKOPF, UTE KRAUS, and HANNS RUDER
University of Tübingen

We demonstrate that a photo-realistic image of a rapidly moving object is dominated by the searchlight and Doppler effects. Using a photon-counting technique, we derive expressions for the relativistic transformation of radiance. We show how to incorporate the Doppler and searchlight effects in the two common techniques of special relativistic visualization, namely ray tracing and polygon rendering. Most authors consider geometrical appearance only and neglect relativistic effects on the lighting model. Chang et al. [1996] present an incorrect derivation of the searchlight effect, which we compare to our results. Some examples are given to show the results of image synthesis with relativistic effects taken into account.

Categories and Subject Descriptors: I.3.7 [**Computer Graphics**]: Three-Dimensional Graphics and Realism—*Color, shading, shadowing, and texture*; J.2 [**Computer Applications**]: Physical Sciences and Engineering—*Physics*

General Terms: Algorithms, Theory

Additional Key Words and Phrases: Aberration of light, Doppler effect, illumination, Lorentz transformation, searchlight effect, special relativity

1. INTRODUCTION

Einstein's Theory of Special Relativity is widely regarded as a difficult and almost incomprehensible theory. One important reason for this is that the properties of space, time, and light in relativistic physics are totally different from those in classical, Newtonian physics. In many respects they

This work was supported by the Deutsche Forschungsgemeinschaft (DFG), and is part of the project D4 within the Sonderforschungsbereich 382
Authors' address: Theoretical Astrophysics, University of Tübingen, Auf der Morgenstelle 10, Tübingen, D-72076, Germany

are contrary to human experience and everyday perception, which is based on low velocities.

Mankind is limited to very low velocities compared to the speed of light. For example, the speed of light is a million times faster than the speed of an airplane and 40,000 times faster than the speed at which the space shuttle orbits the earth. Even in the long term, there is no hope of achieving velocities comparable to the speed of light. Computer simulations are the only means of visually exploring the realm of special relativity, and thus can help the intuition of physicists.

The visual appearance of rapidly moving objects shows intriguing effects of special relativity. Apart from a previously disregarded article by Lampa [1924] about the invisibility of the Lorentz contraction, the first solutions to this problem were given by Penrose [1959] and Terrell [1959]. Various aspects were discussed by Weisskopf [1960]; Boas [1961]; Scott and Viner [1965]; Scott and van Driel [1970]; and Kraus [2000].

Hsiung and Dunn [1989] were the first to use advanced visualization techniques for image shading of fast moving objects. They propose an extension of normal three-dimensional ray tracing. Hsiung and Thibadeau [1990] and Hsiung et al. [1990a] add the visualization of the Doppler effect. Hsiung et al. [1990b] and Gekelman et al. [1991] describe a polygon rendering approach based on the apparent shapes of objects as seen by a relativistic observer. Polygon rendering was also used as a basis for a virtual environment for special relativity [Rau et al. 1998; Weiskopf 1999].

Most authors concentrate their efforts on geometrical appearance and, apart from the Doppler effect, neglect relativistic effects on the lighting model. Chang et al. [1996], however, present a complete description of image shading which takes relativistic effects into account. We agree with most parts of their article, but would like to correct their derivation of the relativistic transformation of radiance. We show how the correct transformation of radiance fits in their shading process. The combination of Chang et al.'s work and this article gives a comprehensive presentation of special relativistic rendering.

We demonstrate that a photo-realistic image is dominated by the searchlight and Doppler effects, which are greatly underestimated when we view the examples given by Chang et al. The Doppler effect causes a shift in wavelength of the incoming light, which results in a change of color. The searchlight effect increases the apparent brightness of the objects ahead when the observer approaches these objects at high velocity. The Doppler effect, the relativistic aberration of light, and time dilation, among others, contribute to the searchlight effect.

2. DERIVATION OF THE TRANSFORMATIONS

2.1 The Transformation of Radiance

The following derivation of the searchlight effect is based on a photon-counting technique. A similar approach can be found in articles by Peebles and Wilkinson [1968]; McKinley [1979; 1980]; and Kraus [2000].

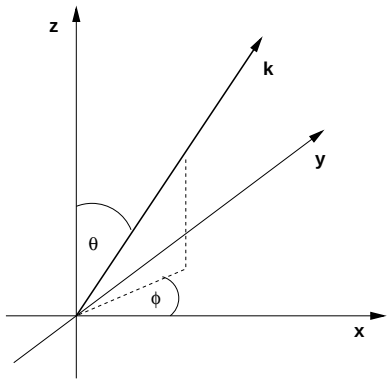

Fig. 1. A photon with wave vector $\vec{k}$.

Consider two inertial frames of reference S and S', with S' moving with velocity v along the z axis of S. Suppose the observer O is at rest relative to S and the observer O' is moving with speed v along the z axis of S. The usual Lorentz transformation along the z axis connects frames S and S'.

In reference frame S, consider a photon with circular frequency ω, wavelength λ, energy E, and wave vector $\vec{k} = (\omega \sin\theta \cos\phi,\ \omega \sin\theta \sin\phi,\ \omega \cos\theta)/c$ with spherical coordinates θ and ϕ, as shown in Figure 1.

In frame S', the circular frequency is ω', the wavelength is λ', the energy is E', and the wave vector is $\vec{k'} = (\omega' \sin\theta' \cos\phi',\ \omega' \sin\theta' \sin\phi',\ \omega' \cos\theta')/c$. The expressions for the Doppler effect and the aberration connect these two representations, cf., McKinley [1979] and Møller [1972]:

$$\lambda' = \lambda D \tag{1}$$

$$\omega' = \omega / D \tag{2}$$

$$E' = E / D \tag{3}$$

$$\cos\theta' = \frac{\cos\theta - \beta}{1 - \beta\cos\theta} \tag{4}$$

$$\phi' = \phi \tag{5}$$

$$D = \frac{1}{\gamma(1 - \beta\cos\theta)} \tag{6}$$

where D is the Doppler factor, $\gamma = 1/\sqrt{1 - \beta^2}$, $\beta = v/c$, and c is the speed of light.

Radiance is the radiant power per unit of foreshortened area emitted into a unit solid angle. A detector at rest in S measures the energy-dependent radiance

$$L_E(\theta, \phi) = \frac{d\Phi}{dE\, dA_\perp\, d\Omega}$$

where Φ is the radiant power or radiant flux, E is the energy, $d\Omega$ is the solid angle, and $dA_\perp$ is the area dA of the detector projected along the radiation direction (θ, ϕ). The radiant flux Φ is the radiant energy per unit time. Accordingly, the wavelength-dependent radiance is

$$L_\lambda(\theta, \phi) = \frac{d\Phi}{d\lambda\, dA_\perp\, d\Omega} \tag{7}$$

with the wavelength λ.

In reference frame S, consider a group of photons, dN in number, with energies between E and $E + dE$ and propagation directions in the element of solid angle $d\Omega$ around (θ, ϕ). Here, the energy-dependent radiance is

$$L_E(\theta, \phi) = \frac{dN\, E}{dE\, dA_\perp\, d\Omega\, dt}$$

or

$$dN = \frac{L_E(\theta, \phi)}{E} dE\, dA_\perp d\Omega\, dt$$

We choose the area dA to be perpendicular to the z axis, so that

$$dA_\perp = dA \cos\theta$$

The z component of the velocity of the photons is $c\cos\theta$. The photons passing dA between time t_0 and time $t_0 + dt$ are contained in the shaded volume dV in Figure 2:

$$dV = dA\, dt\, c \cos\theta$$

Consider another area $d\tilde{A}$ with the same size and orientation as dA. Still in reference frame S, suppose $d\tilde{A}$ is moving with velocity v along the z axis. The photons passing $d\tilde{A}$ between t_0 and $t_0 + dt$ are contained in the shaded volume in Figure 3:

$$d\tilde{V} = dA\, dt(c \cos\theta - v) = \frac{\cos\theta - \beta}{\cos\theta} dV$$

The ratio of the number of photons passing $d\tilde{A}$ in the time interval dt and the number of photons passing dA is the same as the ratio of the volume $d\tilde{V}$ and the volume dV:

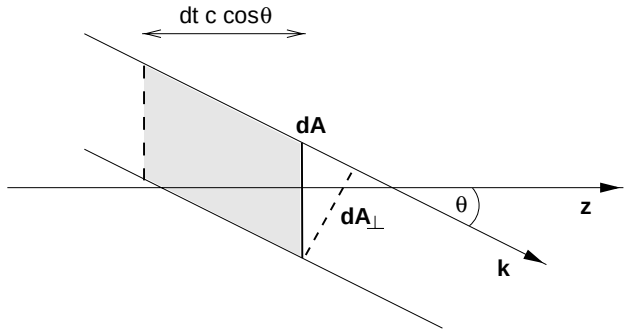

Fig. 2. Photons with propagation direction along the wave vector $\vec{k}$. The area of the detector is denoted dA and is perpendicular to the z axis; $dA_\perp$ is the projection of dA along the radiation direction. The shaded volume dV contains the photons passing dA between time t_0 and time $t_0 + dt$.

$$d\tilde{N} = \frac{L_E(\theta, \phi)}{E}\, dE\, d\Omega\, dt\, \cos\theta\, d\tilde{A}\, \frac{\cos\theta - \beta}{\cos\theta} \tag{8}$$

Now consider the same situation in reference frame S'. The area $d\tilde{A}$ is at rest in S'. The time interval is

$$dt' = dt/\gamma \tag{9}$$

The number of photons counted does not depend on the frame of reference, i.e.,

$$d\tilde{N} = d\tilde{N}' = \frac{L'_{E'}(\theta', \phi')}{E'} dE' d\Omega' dt' \cos\theta' d\tilde{A}' \tag{10}$$

From Eqs. (8) and (10), we obtain

$$\frac{L_E(\theta, \phi)}{L'_{E'}(\theta', \phi')} = \frac{E}{E'} \frac{dE'}{dE} \frac{d\Omega'}{d\Omega} \frac{dt'}{dt} \frac{\cos\theta'}{\cos\theta - \beta} \frac{d\tilde{A}'}{d\tilde{A}} \tag{11}$$

Since the area $d\tilde{A}$ is perpendicular to the separating velocity, it is not changed by Lorentz transformations:

$$d\tilde{A}' = d\tilde{A} \tag{12}$$

With Eqs. (4) and (5), the transformed solid angle is

$$\frac{d\Omega'}{d\Omega} = \frac{\sin\theta'}{\sin\theta} \frac{d\theta'}{d\theta} = \frac{d(\cos\theta')}{d(\cos\theta)} = \frac{1}{\gamma^2(1 - \beta\cos\theta)^2} = D^2 \tag{13}$$

Using Eqs. (3), (4), (9), (12), (13), and (11), we obtain

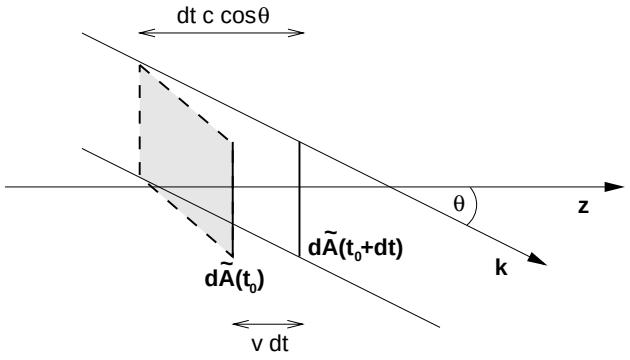

Fig. 3. Photons with propagation direction along the wave vector $\vec{k}$. The area $d\tilde{A}$ moves with velocity v along the z axis. The shaded volume $d\tilde{V}$ contains the photons passing $d\tilde{A}$ between t_0 and $t_0 + dt$.

$$\frac{L_E(\theta, \phi)}{L'_{E'}(\theta', \phi')} = D^3 = \frac{E^3}{E'^3}$$

With the relation between energy and wavelength,

$$\lambda = \frac{hc}{E}, \quad d\lambda = -\frac{hc}{E^2} dE$$

and with

$$L_\lambda(\theta, \phi)|d\lambda| = L_E(\theta, \phi)|dE|$$

we get

$$L_\lambda(\theta, \phi) = L_E(\theta, \phi)\frac{E^2}{hc}$$

Ultimately, then, the transformation expression for the wavelength-dependent radiance is

$$\frac{L_\lambda(\theta, \phi)}{L'_{\lambda'}(\theta', \phi')} = D^5 \tag{14}$$

The transformation law for the following integrated quantity is easily obtained from this equation. With the use of Eq. (1), the transformed radiance is

$$L(\theta, \phi) = \int_0^\infty L_\lambda(\theta, \phi) d\lambda = D^4 \int_0^\infty L'_{\lambda'}(\theta', \phi')\, d\lambda' = D^4 L'(\theta', \phi') \tag{15}$$

2.2 Incident Irradiance from a Point Light Source

The measure for radiant power leaving a point light source in an element of solid angle $d\Omega$ and in a wavelength interval is called the wavelength-dependent intensity I_λ:

$$I_\lambda = \frac{d\Phi}{d\Omega\, d\lambda} \tag{16}$$

The wavelength-dependent irradiance E^i_λ is the radiant power per unit area in a wavelength interval:

$$E^i_\lambda = \frac{d\Phi}{dA\, d\lambda} \tag{17}$$

For a surface patch on the object, the wavelength-dependent irradiance $E^{i'}_{\lambda'}$ coming from a moving point light source is

$$E^{i'}_{\lambda'} = \frac{1}{D^5} \frac{\cos \alpha'}{r'^2} I_\lambda \tag{18}$$

with the angle α' between the normal vector to the surface and the direction of the incident photons and with the apparent distance r' of the light source from the surface patch. These quantities are measured in the reference frame of the object, whereas the wavelength-dependent intensity I_λ is measured in the reference frame of the light source. Accordingly, the integrated, wavelength-independent irradiance is

$$E^{i'} = \frac{1}{D^4} \frac{\cos \alpha'}{r'^2} I \tag{19}$$

The derivation of these equations is presented in the Appendix. Observe that for an isotropic point source in one frame of reference, we get an anisotropic source in the other frame of reference due to the implicit angle dependency in the Doppler factor D.

3. COMPARISON WITH DERIVATION BY CHANG ET AL.

Chang et al. [1996] present a complete treatment of relativistic image shading, which contains apparent geometry, the searchlight and Doppler effects, and a detailed description of the shading process. However, their derivation of the transformation properties of radiance is based on mistaken interpretations of the Theory of Special Relativity and leads to a tremendous divergence from our correct results, presented above.

Chang et al. derive their expressions based on the assumption that the same amount of radiant power is emitted from a surface patch on the object and the corresponding surface patch on the apparent surface. Hence, they

compute the relation between the area of the surface patch on the object and the area of the corresponding surface patch on the apparent surface, as well as the relation between the respective normal vectors. They treat the apparent surface as an object at rest with respect to the observer.

Their derivation is not correct for the following reasons:

Radiant power depends on time intervals and on the energy of photons, both of which are subject to Lorentz transformations. These transformations are missing in Chang et al.'s work.

The observer is moving with respect to the surface patch of the object. Approaching the object, the observer's detector sweeps up photons so that the rate at which radiant energy is received is increased by the observer's motion. This increase is absent for radiation from the apparent surface, which is stationary in the observer's rest frame. Chang et al. ignore this effect as well.

In Chang et al.'s Eq. (36), the transformation of a solid angle is not correct. The mistake is in their calculation of the partial derivatives $\partial\Theta'/\partial\Theta$, $\partial\Theta'/\partial\Phi$, $\partial\Phi'/\partial\Theta$, and $\partial\Phi'/\partial\Phi$ with the use of their Eq. (31) for the transformation of the direction of the light ray. Equation (31) is valid for the special case of polar angle $\Theta = \pi/2$ only, and cannot be used to calculate partial derivatives.

Both wavelength and wavelength intervals are subject to Lorentz transformations. When calculating the radiance per wavelength interval in their Eq. (39) from Eq. (38), Chang et al. apply the Lorentz transformation to the wavelength, but not to the wavelength interval.

In their Eq. (38), they ultimately end up with a factor of D in the transformation of radiance, and also in in their Eq. (39) in the transformation of wavelength-dependent radiance, which differs from the correct result by a factor of D^3 and D^4, respectively. Similarly, the calculation of irradiance in their Eq. (46) and of wavelength-dependent irradiance in their Eq. (47) differs from the correct result by the same factor of D^3 and D^4, respectively.

4. THE SHADING PROCESS

The searchlight and Doppler effects can be readily incorporated in the two common techniques of special relativistic visualization, i.e., ray tracing and polygon rendering.

Relativistic ray tracing as described by Hsiung and Dunn [1989] is an extension of normal 3D-ray tracing. The ray starting at the eye point and intersecting the viewing plane is transformed according to special relativity, i.e., the direction of light is turned due to relativistic aberration. At this point the transformed properties of light can be included by calculating the transformed radiance as well as the transformed wavelength.

In this framework it is not sufficient to consider only three tristimulus values, such as RGB, but the wavelength-dependent energy distribution of light has to be taken into account. The spectral energy distribution has to be known over an extensive range so that the Doppler-shifted energy

distribution can be calculated for wavelengths in the visible range. For final image synthesis, the tristimulus values can easily be obtained from the wavelength-dependent radiance that gets to the eye point.

Relativistic polygon rendering is based on the apparent shapes of objects with respect to the observer. The shading process is described by Chang et al. in full detail. In this process, the expressions for irradiance in step (2)(d)(iv) and for the transformation of radiance in step (2)(f) have merely to be replaced by our Eqs. (18) and (14), respectively. The Doppler factor in Eq. (18) depends on the direction of the photons that reach the object and on the relative velocity of the frame of the point light source and the frame of the object, whereas the Doppler factor in Eq. (14) depends on the direction of the photons that reach the observer and on the relative velocity of the frame of the object and of the frame of the observer.

5. EXAMPLES

The appearance of a scene similar to Chang et al.'s STREET in Figures 4 to 7 shows the tremendous effects of the transformation of radiance on image synthesis. These pictures show the apparent geometry and the radiance transformation, but neglect color changes due to the Doppler effect. Since the spectral energy distribution of the light reflected by the objects in the STREET is unknown, we only show gray-scale images that take the total energy of the whole spectral energy distribution into account. In this case, Eq. (15) is applied. If we used a speed as high as Chang et al.'s, $0.99c$, we would not be able to display the high intensities in Figure 7 properly. So we choose a velocity of $0.8c$. These images were generated by using the ray-tracing method described above. The relativistic extensions are implemented into *RayViS* [Gröne 1996], a normal 3D-ray-tracing program.

Figures 8 and 9 show the appearance of the sun moving at a speed of $0.5c$ to illustrate color changes due to relativistic lighting. We used the polygon-rendering technique described above to produce these images. A detailed presentation of the rendering software can be found in our previous work [Rau et al. 1998; Weiskopf 1999].

6. CONCLUSION

We have demonstrated that, aside from the apparent geometry, the searchlight and Doppler effects play dominant roles in special relativistic visualization. Ray tracing and polygon rendering, two standard techniques in computer graphics, can easily be modified and extended to take into account the searchlight and Doppler effects.

The transformation of radiance could serve as an important element in even more sophisticated shading algorithms in order to generate photorealistic and physically correct images of fast moving objects. For example, radiosity could be extended to visualize relativistic flights through stationary scenes.

Fig. 4. Original appearance of the street.

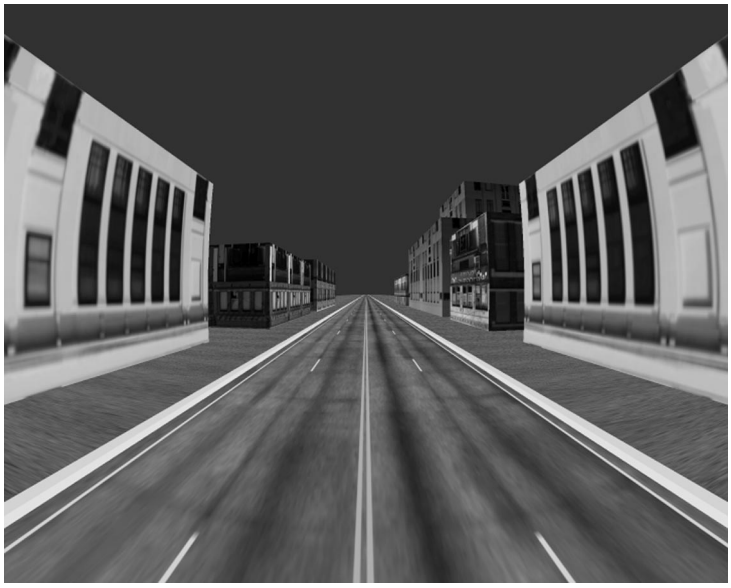

Fig. 5. Appearance of the street with respect to a moving observer. The viewer is rushing into the street with a speed of $0.8c$. The light sources are at rest in the street's coordinate system. The searchlight and Doppler effects are ignored.

Fig. 6. Visualization of the searchlight effect based on the incorrect derivation by Chang et al. The viewer is rushing into the street with a speed of $0.8c$. The light sources are at rest in the street's coordinate system.

Fig. 7. Visualization of the searchlight effect based on the correct Eq. (15) for the transformation of radiance. The difference from Figure 6 is significant. The viewer is rushing into the street with a speed of $0.8c$. The light sources are at rest in the street's coordinate system.

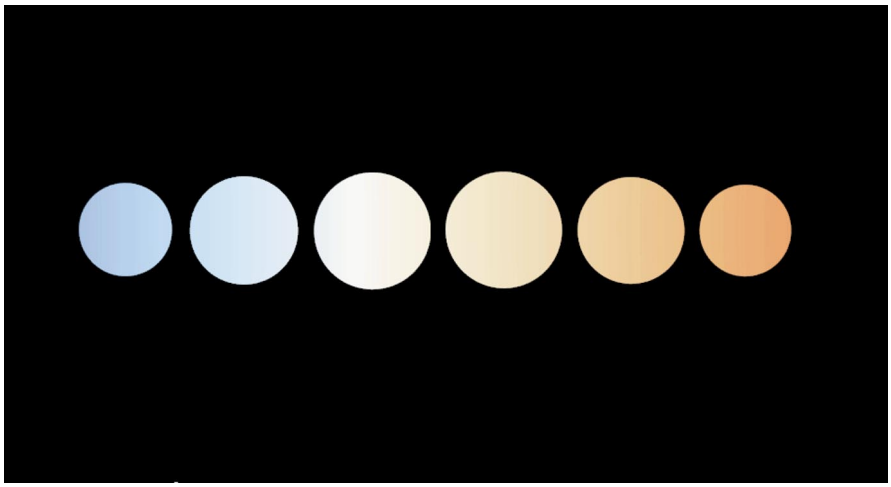

Fig. 8. Visualization of the Doppler effect only: the Doppler-shifted spectral energy distribution is shown with no further transformations. The sun passes by with a speed of $0.5c$. The sun is the only light source and emits blackbody radiation with a temperature of 5762 Kelvin.

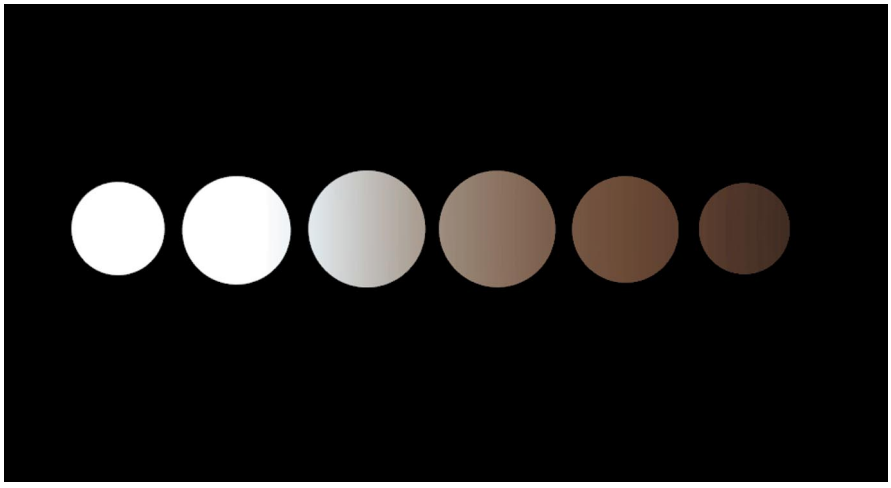

Fig. 9. Visualization of the searchlight and Doppler effects based on Eq. (14). The sun passes by with a speed of $0.5c$. The sun is the only light source and emits blackbody radiation with a temperature of 5762 Kelvin.

APPENDIX

A. INCIDENT IRRADIANCE

The derivation of Eqs. (18) and (19) is presented in this Appendix.

First, consider a finite light source which is at rest in frame S. With Eq. (7), the radiant flux emitted by the light source can be obtained in terms of the wavelength-dependent radiance:

$$d\Phi = L_\lambda \, dA_\lambda^{light} d\Omega^{obj} \, d\lambda \tag{20}$$

where $dA_{\perp}^{light}$ is the area of the projected surface patch of the light source and $d\Omega^{obj}$ is the solid angle of the illuminated surface patch of the object as seen from the position of the light source.

Now consider the same situation in frame S' in which the object is at rest. The radiant flux on the surface patch of the object is

$$d\Phi' = L'_{\lambda'}\, dA_{\perp}^{obj'} d\Omega^{light'}\, d\lambda' \tag{21}$$

with the projected area $dA_{\perp}^{obj'}$ on the object and the solid angle $d\Omega^{light'}$ of the surface patch of the light source as seen from the position of the object. Using Eqs. (14) and (21), we obtain

$$d\Phi' = \frac{1}{D^5} L_{\lambda}\, dA_{\perp}^{obj'} d\Omega^{light'} d\lambda'$$

With the definition in Eq. (17), the incident irradiance emitted from the small solid angle $d\Omega^{light'}$ onto the surface patch of the object is

$$dE_{\lambda'}^{i'} = \frac{d\Phi'}{dA^{obj'} d\lambda'} = \frac{L_{\lambda}}{D^5} \frac{dA_{\perp}^{obj'}}{dA^{obj'}} d\Omega^{light'} \tag{22}$$

The area $dA^{obj'}$ of the surface patch is related to the projected area $dA_{\perp}^{obj'}$ by

$$dA_{\perp}^{obj'} = dA^{obj'} \cos\alpha' \tag{23}$$

with the angle α' between the surface normal and the incident light.

With Eq. (13), the solid angle $d\Omega^{light'}$ is transformed into the frame S of the light source. Furthermore, $d\Omega^{light'}$ is expressed in terms of the projected area on the light source and of the distance between the light source and the surface patch, as shown in Figure 10:

$$d\Omega^{light'} = D^2\, d\Omega^{light} = D^2 \frac{dA_{\perp}^{light}}{r^2} = dA_{\perp}^{light} \left(\frac{D}{r}\right)^2 \tag{24}$$

The light-like connection of the emission event at the light source and the absorption event at the object has the same direction as the wave vector that describes the photons. Therefore, the distance r is transformed in the same way as the circular frequency ω (see Eq. (2)). By following this reasoning or by explicit Lorentz transformation of the separating vector between the emission event and the absorption event, we get

$$r' = r/D \tag{25}$$

Using Eqs. (22), (23), (24), and (25), we obtain the incident wavelength-dependent irradiance originating from a small area of the light source:

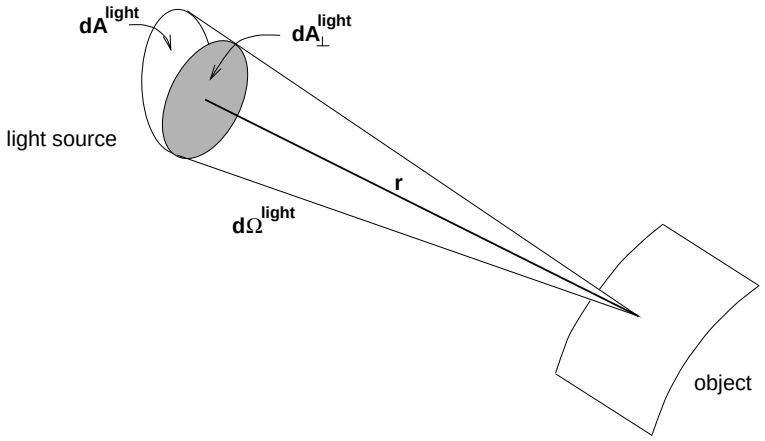

Fig. 10. Geometry of the surface patch of the light source in its rest frame S. The solid angle is given by $d\Omega^{light} = dA_{\perp}^{light}/r^2$. The distance between the light source at emission time and the surface patch of the object at absorption time is denoted r.

$$dE_{\lambda'}^{i'} = \frac{1}{D^5}\frac{\cos\alpha'}{r'^2}L_\lambda \, dA_{\perp}^{light}$$

By integrating over the area of the whole light source, we get the wavelength-dependent irradiance produced by this finite light source:

$$E_{\lambda'}^{i'} = \int \frac{1}{D^5}\frac{\cos\alpha'}{r'^2}L_\lambda \, dA_{\perp}^{light} \tag{26}$$

Now consider a very small, yet finite, light source, described by its wavelength-dependent intensity I_λ. With Eqs. (16) and (20), the wavelength-dependent radiance and the wavelength-dependent intensity from the area $dA_{\perp}^{light}$ are related by

$$dI_\lambda = L_\lambda \, dA_{\perp}^{light} \tag{27}$$

With Eq. (26) and after integrating over the area of the small light source, we find the wavelength-dependent irradiance on the object

$$E_{\lambda'}^{i'} = \int \frac{1}{D^5}\frac{\cos\alpha'}{r'^2}L_\lambda \, dA_{\perp}^{light} = \frac{1}{D^5}\frac{\cos\alpha'}{r'^2}\int L_\lambda \, dA_{\perp}^{light} = \frac{1}{D^5}\frac{\cos\alpha'}{r'^2}I_\lambda$$

This equation even holds for the limit of an infinitesimal light source. Hence we obtain the wavelength-dependent irradiance due to a point light source:

$$E_{\lambda'}^{i'} = \frac{1}{D^5}\frac{\cos\alpha'}{r'^2}I_\lambda$$

Accordingly, the irradiance is

$$E^{i'} = \frac{1}{D^4} \frac{\cos\alpha'}{r'^2} I$$

where I is the intensity of the light source.

REFERENCES

BOAS, M. L. 1961. Apparent shape of large objects at relativistic speeds. *Am. J. Physics 29*, 5 (May), 283–286.

CHANG, M.-C., LAI, F., AND CHEN, W.-C. 1996. Image shading taking into account relativistic effects. *ACM Trans. Graph. 15*, 4 (Oct.), 265–300.

GEKELMAN, W., MAGGS, J., AND XU, L. 1991. Real-time relativity. *Comput. Phys. 5*, 4 (July/Aug.), 372–385.

GRÖNE, A. 1996. Entwurf eines objektorientierten Visualisierungssystems auf der Basis von Raytracing. Ph.D. Dissertation. University of Tübingen, Tübingen, Germany.

HSIUNG, P.-K. AND DUNN, R. H. P. 1989. Visualizing relativistic effects in spacetime. In *Proceedings of the 1989 Conference on Supercomputing* (Reno, NV, Nov. 13–17, 1989), F. R. Bailey, Ed. ACM Press, New York, NY, 597–606.

HSIUNG, P.-K. AND THIBADEAU, R. H. 1990. Spacetime visualization of relativistic effects. In *Proceedings of the 1990 ACM 18th Annual Conference on Computer Science* (CSC '90, Washington, D.C., Feb. 20–22, 1990), A. Sood, Ed. ACM Press, New York, NY, 236–243.

HSIUNG, P.-K., THIBADEAU, R. H., COX, C. B., DUNN, R. H. P., WU, M., AND OLBRICH, P. A. 1990a. Wide-band relativistic Doppler effect visualization. In *Proceedings of the Conference on Visualization '90* (Oct. 1990), 83–92.

HSIUNG, P.-K., THIBADEAU, R. H., AND WU, M. 1990b. T-buffer: Fast visualization of relativistic effects in space-time. *SIGGRAPH Comput. Graph. 24*, 2 (Mar. 1990), 83–88.

KRAUS, U. 2000. Brightness and colour of rapidly moving objects: The visual appearance of a large sphere revisited. *Am. J. Physics 68*, 1 (Jan.), 56–60.

LAMPA, A. 1924. Wie erscheint nach der Relativitätstheorie ein bewegter Stab einem ruhenden Beobachter?. *Z. Physik 27*, 138–148.

MCKINLEY, J. M. 1979. Relativistic transformations of light power. *Am. J. Physics 47*, 7 (July), 602–605.

MCKINLEY, J. M. 1980. Relativistic transformation of solid angle. *Am. J. Physics 48*, 8 (Aug.), 612–614.

MØLLER, C. 1972. *The Theory of Relativity*. 2nd ed. Clarendon Press, New York, NY.

PEEBLES, P. J. E. AND WILKINSON, D. T. 1968. Comment on the anisotropy of the primeval fireball. *Phys. Rev. 174*, 5 (Oct.), 2168.

PENROSE, R. 1959. The apparent shape of a relativistically moving sphere. *Proc. Cambridge Philos. Soc. 55*, 137–139.

RAU, R. T., WEISKOPF, D., AND RUDER, H. 1998. Special relativity in virtual reality. In *Mathematical Visualization*, H.-C. Hege and K. Polthier, Eds. Springer-Verlag, Heidelberg, Germany, 269–279.

SCOTT, G. D. AND VAN DRIEL, H. J. 1970. Geometrical appearances at relativistic speeds. *Am. J. Physics 38*, 8 (Aug.), 971–977.

SCOTT, G. D. AND VINER, R. R. 1965. The geometrical appearence of large objects moving at relativistic speeds. *Am. J. Physics 33*, 7 (July), 534–536.

TERRELL, J. 1959. Invisibility of the Lorentz contraction. *Phys. Rev. 116*, 4 (Nov.), 1041–1045.

WEISKOPF, D. 1999. An immersive virtual environment for special relativity. Report Nr. 108, SFB 382. University of Tübingen, Tübingen, Germany. http://www.uni-tuebingen.de/uni/opx/reports/weiskopf_108.ps.gz.

WEISSKOPF, V. F. 1960. The visual appearance of rapidly moving objects. *Physics Today 13*, 9, 24–27.

Received: April 1998; revised: April 1999; accepted: April 1999